IMPROVEMENTS TO THE STACKTAIL AND DEBUNCHER MOMENTUM COOLING SYSTEMS*

V. Lebedev†

Fermilab, Batavia, IL 60510, U.S.A.

Abstract

Upgrades and improvements to the stacktail and Debuncher momentum cooling systems have contributed to the success of Tevatron Run II. This paper describes measurements and simulations that facilitated achievement of peak stacking rates of $30{\cdot}10^{10}$ hour^{-1} as well as a better understanding of the principles of the system design and operation. The heating of the antiproton core by the stacktail system is a serious limiting factor to the maximum stacking rate. The paper also discusses heating mechanisms and ways to mitigate them.

INTRODUCTION

Antiprotons are produced by a 120 GeV Main Injector proton beam hitting the antiproton production target every 2.2 s. The antiprotons coming out of the target are focused by the lithium lens to the AP-2 line and transported to the Debuncher where they are stochastically precooled. They are then transferred to the Accumulator where they are momentum-cooled into a dense core by stochastic cooling systems. The stacking rate decreases with stack size, therefore after achieving a stack size of about $30{\cdot}10^{10}$ antiprotons, they are transferred to the Recycler. In the Recycler, the antiprotons are cooled using both stochastic and electron cooling, to be used for collider operations.

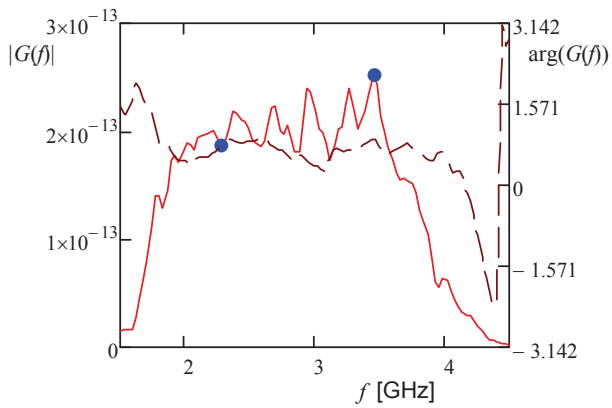

Figure 1: Dependence of the magnitude and phase of the total stacktail gain on frequency after equalizer installation for the revolution frequency 628830 Hz.

The sequence of upgrades carried out over the last 3 years and their results are presented in Refs. [1] and [2]. Here we mention only two the most important ones: a correction of the system gain with an equalizer and an increase of the lattice slip factor [4]. The magnitude and phase of the total stacktail gain after the equalizer installation are shown in Figure 1. The slip factor increase resulted in the bands being close to overlap at the high frequency end. The upgrades resulted in an increase of the peak stacking rate from $20{\cdot}10^{10}$ to $30{\cdot}10^{10}$ hour^{-1}. That is quite close to expectations based on model prediction. Recent developments of the stochastic cooling theory [3, 4] have been extremely useful in choosing the upgrade path and to follow up the problems encountered along the way. In this paper we discuss the present stacking rate limitations and possible ways to overcome them.

STACKING IN THE ACCUMULATOR

Figure 2 presents measured and simulated particle distributions during the first 100 s of stacking in the Accumulator. The measurements were performed by recording the beam Schottky noise of the longitudinal Schottky monitor operating at the 126th harmonic of the revolution frequency (~79 MHz). The signal was mixed down and digitized during the 100 s period by an 8 bit digital scope with a sampling rate of 156 kHz. The data were split into arrays belonging to different stacking cycles (2.2 s long). Then, each stacking cycle data were additionally split into 160 arrays with a length of 2048 words and subjected to the FFT. Averaging 16 consecutive spectra resulted in 10 Schottky noise spectra per stacking cycle. A low pass filter installed before the digitizer reduced the core signal and allowed us to achieve the required dynamic range with only an 8 bit scope resolution. The effect of the filter is visible in Figure 2 as a noise floor that increases with frequency.

The stacking process has the following steps. First, antiprotons precooled in the Debuncher are transferred to the Accumulator. They arrive at the deposition orbit with a revolution frequency of 628756 Hz. There are ~$2.3{\cdot}10^{8}$ antiprotons in one transfer with rms revolution frequency spread of 3 Hz. Then, the injected antiprotons are RF displaced to the deposition frequency of 628831 Hz. The width of the RF bucket is chosen to maximize the stacking rate. This results in about ~2% of the injected particles being left at the deposition orbit. They are presented as a small peak in the spectrum at the frequency of 628750 Hz. The large peak represents the injected beam. The stacktail system pulls the injected particles into the core located at 628897 Hz. One can see a step by step propagation of particles to the core in Figure 2. The particles which were not moved out of the deposition region before the next pulse arrives are RF displaced in

* Work supported by the U.S. Department of Energy under contract No. DE-AC02-76CH03000

† val@fnal.gov

the direction of the injection orbit and lost for further stacking. One can see the build-up of such particles on the left from the deposition orbit. Experiments show that a higher stacking rate is achieved if the stacktail is on during RF displacement of the beam from the injection to the deposition orbit. The presence of RF strongly distorts the Schottky spectra making the last spectrum of each stacking cycle unusable for analysis (0.22 s out of 2.2 s.)

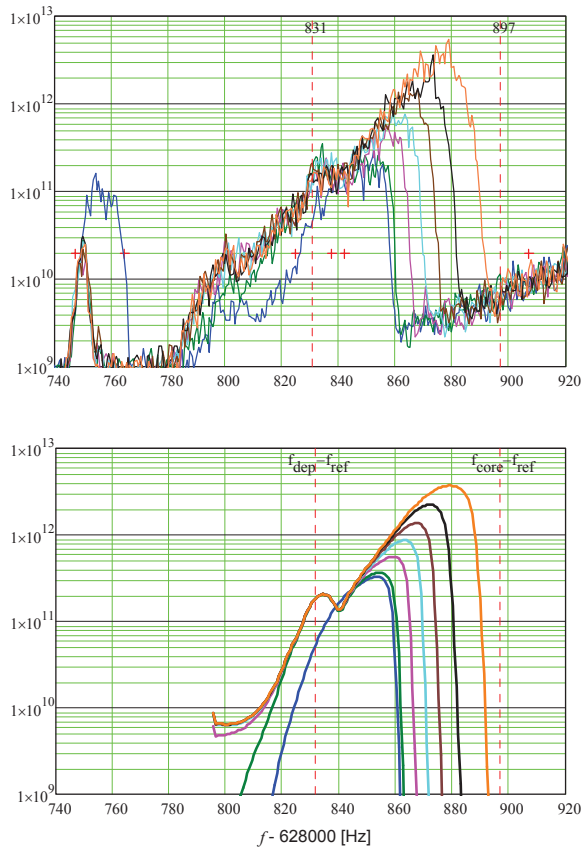

Figure 2: Evolution of particle distribution over revolution frequency during the first 100 s of stacking; top - measurements, bottom - simulations. Curves are built at 1.54 s in cycle 2, and 0.22 s in cycles 3,5,8,13,23 and 47.

The major goal of the measurements presented in Figure 2 was to make a direct measurement of the system gain. Previous measurements [4] were performed with narrow momentum spread, low intensity beams. They provided a measurement of gain dependence on frequency and beam momentum with good accuracy (≤10%) and resulted in a credible model which guided us through the upgrades. However, it was impossible to measure the absolute value of the gain with comparable accuracy because we could not control or measure with sufficient accuracy the longitudinal distribution of this narrow beam. One can see a good correlation between the measurements and simulations in Figure 2. The only free parameter in the model was the absolute value of the gain.

The simulations are based on solving the Fokker-Planck equation where all system parameters came from the beam-based measurements [4]. To accelerate the simulations, we presently neglect in calculations the particle interaction through the cooling system, which modifies the cooling force and diffusion. That allowed us to simulate a complete 1 hour stacking cycle in about 20 minutes on a single-processor computer. Correct accounting of the particle interaction would increase computational time by at least 2 or 3 orders of magnitude resulting in a many hour simulation on a multiprocessor computer. There are a few reasons which make simulations so extensive. First, in contrast to a normal stochastic cooling system where computation of a single cooling cycle completely characterizes the system, characterization of the stacktail system requires simulations of about 1000 cycles. It lengthens computations proportionally. Second, taking into account the particle interaction for the stacktail requires much more computations than for a general cooling system where this interaction is only important at the end of the cooling cycle. In this case the band overlap can be neglected and a computation of beam dielectric functions for all harmonics requires a computation of single integral over the distribution function:

$$\varepsilon_n(y)=\begin{cases}1+\dfrac{G_{PC}(\omega_n)}{2\pi i\eta n}\displaystyle\int_{\delta\to 0_+}\frac{x\,d\psi_0(x)/dx}{x-y-i\delta}dx\,, \\ 1+\dfrac{1-A(\omega)e^{-i\omega T_0}}{2\pi i\eta n}G_{FC}(\omega_n)\displaystyle\int_{\delta\to 0_+}\frac{d\psi_0(x)/dx}{x-y-i\delta}dx\,.\end{cases} \quad (1)$$

Here the top and bottom equations correspond to the cases of the Palmer and filter cooling, with their gains parameterized as follows: $G_{PC}(x,\omega_n)=xG_{PC}(\omega_n)$ and $G_{FC}(x,\omega_n)=G_{FC}(\omega_n)$, $A(\omega)$ describes the depth and dispersion of the notch filter, η is the slip factor, T_0 is the revolution time, and $y=-(\omega-n\omega_0)/n\eta$. In contrast, the stacktail operates very close to band overlap. That requires using an expression which takes into account the band overlap in computations of the dielectric function[1] [3]:

$$\varepsilon(\omega)=1+\left(1-A(\omega)e^{-i\omega T_0}\right)\int_{\delta\to 0_+}\frac{d\psi_0(x)}{dx}\frac{G(x,\omega)e^{i\omega T_2\eta_2 x}}{e^{i\omega T_0(1+\eta x)}-(1-\delta)}dx\,. \quad (2)$$

This integral differs at different harmonics resulting in the need to make the computation for a large number of harmonics. This drastically increases the time of computation. To demonstrate the strength of band overlap effect, the dielectric functions and stability diagrams computed with and without it taken into account are presented in Figure 3. For both cases, the wiring of the system (multiple pickup legs and notch filters) was correctly accounted [4]. One can see that the difference is close to the total value of the effect. In particular, ignoring the band overlap results in a decrease of the stability region by almost a factor of 2. Thus if one wants to have a correct accounting of signal suppression, it has to be done with band overlap taken into account. This left us with no choice but to neglect the signal particle interaction in solving the Fokker-Planck equation. To estimate the effect of particle interaction on the computation results, ε

[1] Eq. (2) is justified for the case of a system with one pickup leg and one notch filter. Taking into account multiple legs and notch filters would make this equation lengthier and therefore we omit it. A corresponding expression is presented in Ref. [4].

was computed for a number of time steps and frequencies after a solution of the Fokker-Plank equation is obtained. Figure 4 presents the changes in ε within the time of cycle 47 (~103 s) for the simulations presented in Figure 2. The beam is close to the stability boundary at the beginning of the cycle when the injected beam has narrow distribution; but in 100 ms smoothening the beam distribution in the vicinity of the deposition orbit results in a reduction of particle interaction by more than a factor of two. Consequently, as long as the stack size is small, the effect of particle interaction is also small during most of cycle time resulting in relatively small (≤10-20%) overall correction for the stacking rate. Figure 4 also shows that in the stacktail region (628840-628890 Hz) the $|\varepsilon$ -1| does not exceed 0.25, i.e. the particle interaction has a small effect on the speed of the stack front propagation and, consequently, on the value of the gain deduced from the experimental data. Note that for a well-tuned cooling system, its operation in a regime with strong particle interaction also implies that the system operates close to its optimal gain, when the particle heating power due to diffusion is equal to half of the cooling power due to cooling force. In this case the signal suppression (amplification) due to particle interaction reduces (increases) both the cooling force and diffusion yielding a comparatively small effect of the particle interaction if $|\varepsilon - 1| \le 0.5$.

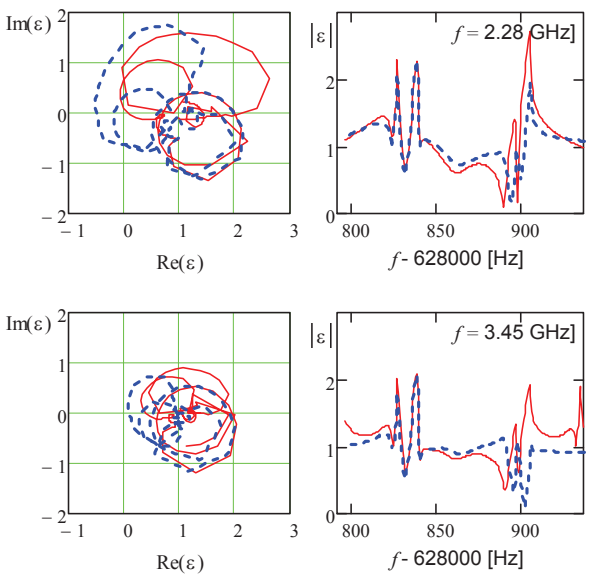

Figure 3: The beam stability diagrams (left) and the dependencies of $|\varepsilon|$ on the revolution frequency (right) computed at 55 ms of stacking cycle 800 for different revolution frequency harmonics: top - n=3626 (2.28 GHz), bottom - n=5486 (3.45 GHz); red solid lines – computed with band overlap taken into account, blue dashed lines –band overlap is neglected.

Further accumulation of antiprotons results in an increased contribution of core particles to the dielectric function, so that it will be making a dominant contribution after approximately 500 cycles (20 min). In this case the particle interaction for the core is strong during the entire cycle and cannot be neglected. Figure 3 presents a comparison of contributions for the particles in the core and fresh beam delivered to the deposition orbit.

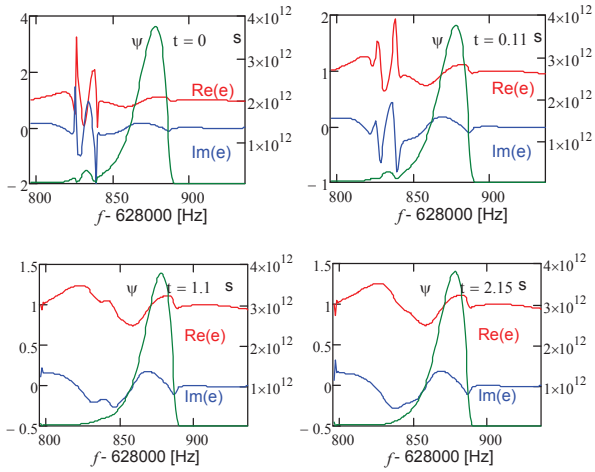

Figure 4: The real (red) and imaginary (blue) parts of ε computed at different times in cycle 47 for stacking simulations presented in Figure 2. The particle distribution is shown with a dark green line.

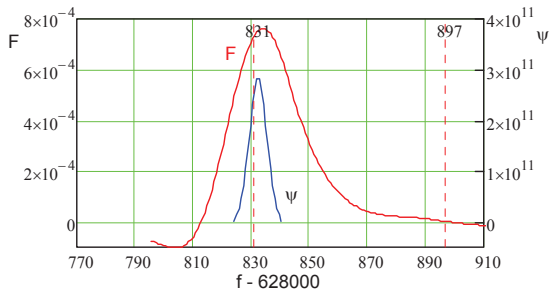

Figure 5: Dependences of cooling force and the distribution of particles delivered to the deposition orbit on the revolution frequency.

Both the experimental data and simulations presented in Figure 2 show that the stacktail is not capable of clearing the deposition orbit before next pulse arrival. It is mainly related to the narrow flattop of the cooling force as can be seen in Figure 5. Both the simulations and experimental results show that the optimum deposition orbit is in the vicinity of 628831 Hz or, as the simulations show, at a frequency slightly below the frequency where the cooling force achieves its maximum. This results in the low frequency tail of the beam delivered to the deposition orbit seeing about half of the cooling force. Consequently, a significant fraction of these particles do not clear the deposition orbit before the next pulse arrives and is lost.

The present model, where the particle interaction through the stacktail is not taken into account, yields that the stacking rate continues to grow with a decrease in momentum spread. However, as shown above, the system is close to the stability boundary and it is unclear how such decrease can affect the stacking rate. Recent reductions in the Debuncher beam momentum spread by about 10% yielded a ~5-10% increase in stacking rate.

This suggests that a further decrease should result in an increase in stacking rate. If required, the system stability can be supported by ramping the stacktail gain within stacking cycles.

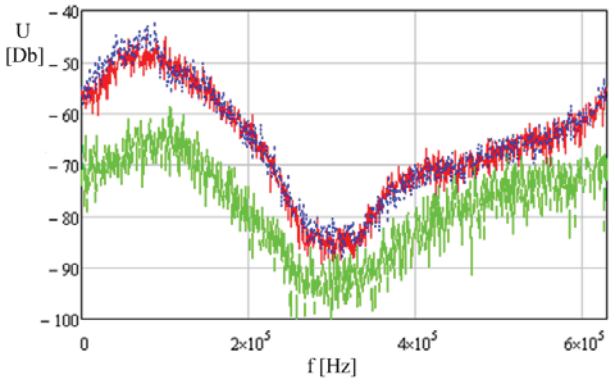

Figure 6: Spectral density for stacktail TWT 16; green line – no stacking, blue line – beginning of the stacking cycle, red line – end of the stacking cycle.

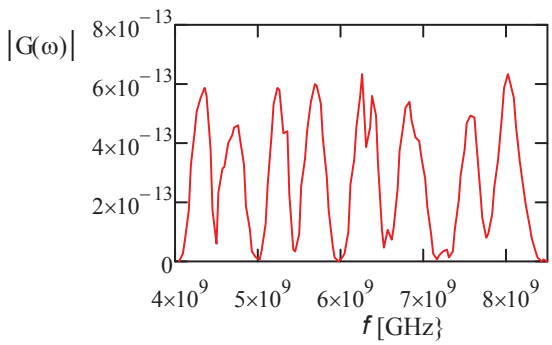

Figure 7: The dependence of gain on frequency for Debuncher longitudinal cooling.

Another problem affecting stacktail operation is related to the intermodulation signal distortion (IMD) by TWTs. It reduces the depth of the notch introduced by the notch filters on harmonics of the core particles resulting in core heating. Figure 6 presents a typical spectral power for one of the revolution harmonics. The green line corresponds to the case of no stacking. In this case, the noise consists of two contributions: the thermal noise of preamplifiers and the noise of the core particles. Both are shaped by the notch filters. It is unclear whether the minimum spectral density is determined by the noise floor of the spectrum analyzer, by TWT noise or by something else; but in the absence of IMDs, this value should not change when stacking is resumed. The red and blue curves represent the spectral density during stacking. One can see that stacking results in a 10 Db increase in the spectral density on the core due to IMDs. The measurements were performed for all TWTs. They showed that IMDs are larger at high frequencies and that they are different for different TWTs. The notch depth (ratio of maximum to minimum spectral densities) drops from 31-37 Db range at 2.4 GHz to 22-28 Db at 3.5 GHz. Figure 6 also demonstrates that the notch depth hardly depends on the stacktail power in the range of operational power variations (~6 Db). Simulations show that if the spectral density of the kicker voltage was determined by thermal and particle noise, the notch depth would be about 20 Db deeper. Core heating by IMDs necessitates gain reduction with increased stack size to prevent longitudinal core blowup. It results in a reduction of stacking rate with stack size. This additional heating due to IMDs was taken into account in the numerical model described above resulting in reasonable agreement between simulations and measurements.

DEBUNCHER LONGITUDINAL COOLING

In contrast with the Accumulator, where all stochastic cooling systems operate close to the optimum gain, all Debuncher systems are power limited during most of the cooling cycle. In this case, the cooling decrement has comparatively weak dependence on the effective bandwidth of the system. Instead of growing as W^2 it grows proportionally to $\sqrt{W}$ resulting in that the bandwidth increase yields four times smaller gain than for a system operating close to the optimal gain. Analysis of possible equalization schemes revealed that only a few percent cooling rate improvement could be achieved. Therefore, we did not pursue this option.

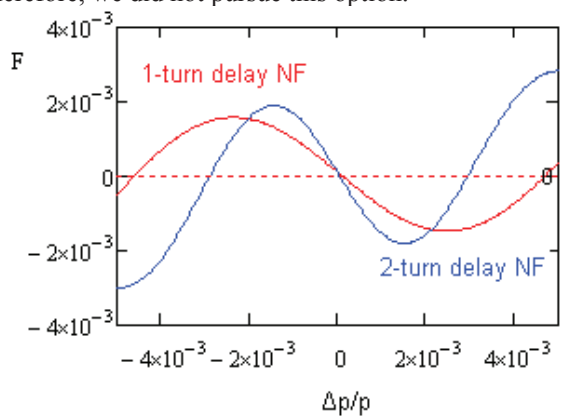

Figure 8: Dependence of cooling force on momentum for one-turn and two-turn delay notch filters in Debuncher.

Longitudinal Debuncher cooling is a filter cooling system with its frequency band split into four sub-bands whose signals are wired through a common notch filter. Each band has 2 additional pickup sub-bands combined into a kicker band. Figure 7 presents the gain of the system reconstructed from measurements of each sub-band. To improve the longitudinal cooling, we made an upgrade of its notch filter; so that during the first half of the cooling cycle the long leg of the notch filter has one turn delay (as before the upgrade) and in the second half of the cycle the delay is switched to two turns. It effectively doubles the small amplitude cooling rate for the same electronic gain. The two-turn delay notch filter also reduces the momentum acceptance of the cooling system. However, it is engaged after 1 s of normal cooling, when the beam is already sufficiently cold. Therefore, switching in the two-turn delay notch filter improves momentum cooling while not causing additional

particle loss from the distribution tails. Figure 8 presents the cooling force for the cases of one and two-turn delay notch filters computed from the measured beam response functions. Engaging the two-turn notch filter effectively increases the power of the system by a factor of 4 and results in the system staying on the optimum gain for the second half of the cooling cycle. The optimum gain is proportional to the square of beam momentum spread. Therefore, to stay at optimal gain, the gain is gradually decreased by 6 Db to the end of the cooling cycle.

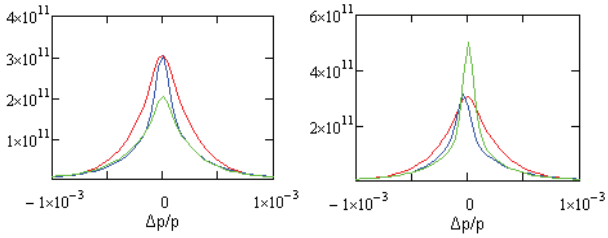

Figure 9: Simulated distortion of the Schottky spectrum at the end of Debuncher cooling cycle depending on the value of $\delta A = A - 1$: red lines - undistorted spectrum, blue line (left) - $\delta A = 0$; green line (left) - $\delta A = -0.05$, blue line (right) - $\delta A = 0.05i$; green line (right) - $\delta A = 0.05$.

Computer simulations have been based on solving the Fokker-Planck equation [3] with measured cooling system parameters. Taking into account that the particle interaction is important only at the end of the cooling process, ε was computed neglecting band overlap using the bottom equation of Eq. (1). The computation of the integral over the distribution function was reduced to a matrix multiplication to accelerate the computations. It can be presented in the following form:

$$\varepsilon(\omega_k, x_n) = 1 + \left(1 - A(\omega_k) e^{-i\omega_k T_0}\right) G(\omega_k) \Xi_{nm} \psi_m , \qquad (3)$$

where indices n and m numerate dependencies on the momentum, index k numerates the revolution frequency harmonics, and we omitted the time dependent index. Matrix Ξ_{nm} is computed once at the beginning of calculations. It was obtained by a piece-wise integration of the distribution interpolated by the second order polynomial between nodes. That yields:

$$\Xi_{nm} = a(n-m+1) - a(n-m-1) + b(n-m+1) + b(n-m-1) - 2b(n-m) , \qquad (4)$$

$$a(n) = \frac{1}{2}\ln\left(\frac{k+1/2}{k-1/2}\right), \quad b(n) = n\ln\left(\frac{k+1/2}{k-1/2}\right) - 1 .$$

The integral ($\Xi_{nm}\psi_m$) was computed once at every time step resulting in fast computations of $\varepsilon(\omega_k, x_n)$ for multiple revolution frequency harmonics. Because the cooling system has 8 sub-bands its gain oscillates repeatedly with frequency (see Figure 7). To achieve an accurate description, 120 harmonics uniformly distributed through its frequency band are used.

Simulations predicted ~10% improvement in beam momentum spread at the end of cooling cycle with the installation of the two-turn delay notch filter. The observed cooling improvement is in agreement with numerical simulations. The final rms momentum spread is $3.2 \cdot 10^{-4}$. The simulations also proved that the result depends strongly on the notch depth of the filter. Therefore special attention was paid to amplitude balancing of the notch filter legs. Although predicted and measured evolutions of the distribution are quite close, there are still minor inconsistencies. In particular, there is a difference in the signal suppression by the cooling system. The spectral density measured from the cooling pickup is:

$$S_n(y) \propto \psi_0(y) \Big/ \left|\varepsilon_n(y)\right|^2 . \qquad (5)$$

As it follows from Eq. (1), there is no signal suppression in the distribution center for a perfect notch filter, $A(\omega)=1$. However the notch filter of Debuncher longitudinal cooling is far from being perfect. The rms value of $\delta A_n = \left|A(\omega_n) - 1\right|$ weighted with the system gain is equal to 0.08. Figure 9 presents possible spectrum distortions depending on δA_n for a given harmonic. One can see that that the real part of δA results in the signal suppression or amplification depending on its sign, while the imaginary part shifts the spectrum. The reason that there are discrepancies between the measurements and simulations is not quite clear. A systematic offset in measuring the real part of $A(\omega)$ is the most probable one.

DISCUSSION

Improvements to the stacktail and Debuncher momentum stochastic cooling systems resulted in a stacking rate close to its theoretical limit. Presently, the stacking rate is ~75% of the Debuncher flux. ~5% of the antiprotons are outside of Debuncher cooling range and remain in the Debuncher; ~2% are left at the deposition orbit in Accumulator; and ~15% are back-streamed from the stacktail. The amount of back-streamed particles grows to ~25% at the end of a stacking interval. There has been considerable progress in understanding cooling system operations.

The stacktail numerical model shows that clearing of the deposition orbit is the major limitation in the stacking rate. It predicts that the rest of the stacktail allows significantly larger flux (~20-30%). It is unclear how much stacking can be improved by reducing the momentum spread of injected beam but it looks like as the most promising path to pursue.

The author is grateful to J. Morgan, V. Nagaslaev, R. Pasquinelli, D. Vander Meulen and S. Werkema for their contributions to the development of the stochastic cooling systems described in this paper.

REFERENCES

[1] V. Lebedev, "Status of Tevatron Run II," PAC2009.

[2] R. Pasquinelli, *et al.*, "Progress in Antiproton Production at the Fermilab Tevatron Collider," PAC-2009.

[3] V. Lebedev, "Stochastic Cooling with Schottky Band Overlap," COOL'05, AIP Conf. proc., v. 821, p. 231.

[4] V. Lebedev, "Antiproton accumulation and production," COOL'07, p. 39.